

## Cobalt complexes based on 2-(1H-benzimidazol-2-yl)-phenol derivatives: Preparation, spectral studies, DFT calculations and catalytic behavior toward ethylene oligomerization

Marzieh Haghverdi, Azadeh Tadjarodi, Naeimeh Bahri-Laleh & Mahdi Nekoomanesh Haghghi

To cite this article: Marzieh Haghverdi, Azadeh Tadjarodi, Naeimeh Bahri-Laleh & Mahdi Nekoomanesh Haghghi (2017): Cobalt complexes based on 2-(1H-benzimidazol-2-yl)-phenol derivatives: Preparation, spectral studies, DFT calculations and catalytic behavior toward ethylene oligomerization, Journal of Coordination Chemistry, DOI: [10.1080/00958972.2017.1328506](https://doi.org/10.1080/00958972.2017.1328506)

To link to this article: <http://dx.doi.org/10.1080/00958972.2017.1328506>

 View supplementary material 

 Accepted author version posted online: 08 May 2017.

 Submit your article to this journal 

 View related articles 

 View Crossmark data 

**Publisher:** Taylor & Francis

**Journal:** *Journal of Coordination Chemistry*

**DOI:** <http://dx.doi.org/10.1080/00958972.2017.1328506>

## **Cobalt complexes based on 2-(1H-benzimidazol-2-yl)-phenol derivatives: Preparation, spectral studies, DFT calculations and catalytic behavior toward ethylene oligomerization**

MARZIEH HAGHVERDI<sup>†</sup>, AZADEH TADJARODI<sup>\*†</sup>, NAEIMEH BAHRI-LALEH<sup>‡</sup> and MAHDI NEKOOMANESH HAGHIGHI<sup>‡</sup>

<sup>†</sup>Research Laboratory of Inorganic Materials Synthesis, Department of Chemistry, Iran University of Science and Technology, Tehran, Iran

<sup>‡</sup>Polymerization Engineering Department, Iran Polymer and Petrochemical Institute (IPPI), Tehran, Iran

In this study, five novel Co(II) complexes of 2-(1*H*-benzimidazol-2-yl)-phenol derivatives (HL<sub>x</sub>: x = 1-5) have been synthesized and characterized. The general formula for complexes **C1** and **C2** is K<sub>2</sub>[Co(HL<sub>1,2</sub>)<sub>2</sub>Cl<sub>2</sub>]·H<sub>2</sub>O, for complex **C3** K<sub>2</sub>[Co(HL<sub>3</sub>)<sub>2</sub>Cl<sub>2</sub>], and for complexes **C4** and **C5** [Co(HL<sub>4,5</sub>)<sub>2</sub>]. In all complexes, the ligands are coordinated as bidentate, via one imine nitrogen and the phenolate oxygen atoms. The structures of the compounds were characterized by FT-IR, UV-Vis, <sup>1</sup>H-, <sup>13</sup>C-NMR spectroscopies, ICP and elemental analysis (C, H and N). The purity of these compounds was ascertained by melting point (m.p.) and TLC. Geometry optimization of the studied complexes was done by Gaussian09 software at B3LYP/TZVP level of theory and satisfactory theoretical–experimental agreement was achieved for NMR and IR spectra of the compounds. Based on the combined experimental and theoretical studies, six-coordinate octahedral structures have been proposed for complexes **C1-C3**, while complexes **C4** and **C5** had distorted tetrahedral geometry. All complexes were activated with diethylaluminum chloride (Et<sub>2</sub>AlCl), cobalt(II) complexes containing bulky methyl groups in the aryl moiety show high catalytic activities (1774 kg·mol<sup>-1</sup>(Co)·h<sup>-1</sup>) for ethylene oligomerization. The oligomers obtained from the cobalt complexes exhibit good selectivity for linear 1-butene and 1-hexene. Results revealed that both the steric and electronic effects of ligands strongly affect the catalytic activities and the properties of the catalytic products.

---

\*Corresponding author. Email: [tajarodi@iust.ac.ir](mailto:tajarodi@iust.ac.ir)

*Keywords:* Benzimidazolylphenols; Cobalt(II) complexes; Characterization; DFT calculations; Ethylene oligomerization

## 1. Introduction

$\alpha$ -Olefins are major industrial reactants that are extensively used in the preparation of detergents, lubricants, plasticizers, oil field chemicals, and comonomers used for branched polyolefins [1]. The novel late transition metal catalysts compared with traditional Ziegler-Natta catalysts of early transition metals possess advantages not only in catalytic activity and selectivity, but also in their potential for tolerating heteroatom functionalities [2]. Over the past decade, progress has been made in ethylene reactivity by late-transition metal complex catalysts. Regarding iron and cobalt systems based on bis(arylimino)pyridines, those initially discovered by the groups of Brookhart and Gibson individually are well known [3].

After that, relative research works have been focused on modifying those catalysts' models through synthesizing numerous derivatives of their complexes and also devising alternative models of these catalysts [4]. However, there are few models of iron and cobalt complex catalysts performing good catalytic activities toward ethylene oligomerization and polymerization in comparison with various models of nickel complexes. Among different models of these catalysts, the catalysts containing bi- and tridentate ligands for polymerization and oligomerization of ethylene to  $\alpha$ -olefins has attracted much attention.

Among bidentate ligands, there are reports about the use of benzimidazolyl-phenol and its derivatives as chelating agents with various transition metal complexes [5-10], that as well as having good catalytic activities toward ethylene oligomerization. Studies on characterization of these types of the compounds and their complexes are rather scarce. Therefore, the preparation of these compounds becomes more important [11]. A general method for their synthesis is the condensation of *o*-phenylenediamines with 2-hydroxy aromatic aldehydes [12].

In this work, the synthesis and characterization of the Co(II) complexes with various 1*H*-benzimidazol-2-yl-phenol derivatives are reported. Density functional theory (DFT) calculations of the electronic properties of the compounds were performed which were in good agreement with the experimental results. Also, the catalytic behavior of Co(II) complexes in ethylene reactivity was investigated. Relatively good catalytic activities toward ethylene oligomerization could be observed in the presence of diethylaluminum chloride (Et<sub>2</sub>AlCl).

## 2. Experimental

### 2.1. Chemistry and apparatus

All manipulations of air- and moisture-sensitive compounds were performed under nitrogen using standard Schlenk techniques. Toluene was refluxed over sodium-benzophenone and distilled under nitrogen prior to use. Diethylaluminum chloride ( $\text{Et}_2\text{AlCl}$ ) was purchased from Aldrich Chemicals. All other chemicals were obtained commercially and used without purification. Elemental analyses were carried out in a Perkin Elmer model 2400 series 2 (made in USA) automatic carbon, hydrogen, nitrogen analyzer. Determination of metal percentage was performed using ICP (3410ARL model made in Swiss). NMR spectra (300 MHz for  $^1\text{H}$  and 75 MHz for  $^{13}\text{C}$ ) were run on a Bruker AVANCE-300 instrument (Germany) in dimethylsulfoxide ( $\text{DMSO-d}_6$ ) using tetramethylsilane (TMS) as internal standard. IR spectra were recorded in KBr disks on a Shimadzu FT-IR 8400 spectrometer (Japan) from 400-4000  $\text{cm}^{-1}$ . UV-Vis spectra were taken on a Shimadzu UV-1700 spectrophotometer (Japan) in DMSO solution. GC analyses were performed with a Varian CP-3800 gas chromatograph equipped with a flame ionization detector and a 100 m (0.25 mm i.d., 0.5  $\mu\text{m}$  film thickness) CP-Sil PONA CB. The yield of oligomers was calculated by referencing with the mass of the solvent on the basis of the prerequisite that the mass of each fraction was approximately proportional to its integrated areas in the GC trace. Selectivity for linear 1-alkenes was defined as (amount of linear 1-alkenes of all fractions)/(total amount of oligomer products) in percent. Melting points were determined using an electrothermal melting point apparatus. The completion of reactions was monitored by TLC.

### 2.2. Synthesis of the ligands: General procedure

The  $\text{HL}_1$  to  $\text{HL}_5$  ligands (see scheme 1 for labels) were prepared according to previous literature procedures [13]. In a typical procedure, 2-(5,6-dimethyl-1H-benzimidazol-2-yl)-phenol ( $\text{HL}_5$ ) was obtained by the reaction of 2-hydroxybenzaldehyde (1.83 g, 15.0 mmol) with sodium metabisulfide (1.60 g, 8.5 mmol) at room temperature in 20 mL of ethanol and water, respectively. The reaction mixture was stirred vigorously and more ethanol was added. The mixture was kept in a refrigerator for several hours. Then, it was filtered and sodium hydroxyl-(2-hydroxyphenyl)methansulfonate salt was obtained from the crude extract. This crude salt and

4,5-dimethylbenzene-1,2-diamine (0.54 g, 4.0 mmol) in 10 mL of dimethylformamide (DMF) were refluxed for 4 h at 130 °C in an oil bath. The completion of reaction was monitored by TLC. Then the mixture was poured in an ice bath. After that, the reaction was quenched by adding water and obtained ligand filtered and recrystallized from ethanol. This method was selected because of its ease, high yield and short synthesis time. This intermediate compound (namely, bisulfite compound of the aldehyde) was utilized to catalyze the benzimidazole synthesis since 1,2-phenylenediamine derivatives and aldehydes do not give cyclization reaction by themselves under mild conditions and possibly might lead to Schiff bases. 2-(5,6-Dimethyl-1H-benzimidazol-2-yl)-phenol was used as ligand for the synthesis of the complexes.

### 2.3. Synthesis of the cobalt complexes C1-C5

**2.3.1.  $K_2[Co(HL_1)_2Cl_2] \cdot H_2O$  (C1).** To a schlenk tube that was purged three times with nitrogen, a solution of  $HL_1$  (0.106 g, 0.5 mmol) and KOH (0.028 g, 0.5 mmol) in methanol was added. Then, a solution of  $CoCl_2 \cdot 6H_2O$  (0.059 g, 0.25 mmol) in methanol was added. The color of the solution changed immediately. The reaction mixture was stirred for 24 h at room temperature under nitrogen. Completion of the reaction was monitored by TLC. The resulting precipitation was separated by filtration, washed with diethyl ether and dried in vacuum. Brick red powder, yield: 62%. IR (KBr disc,  $cm^{-1}$ ): 3425  $\nu(N-H)$ , 3180  $\nu(C-H)$ , 1625  $\nu(C=N)$ , 1533  $\nu(C=C)$ , 1247  $\nu(C-O)$ , 667, 574  $\nu(Co-O)$ , 450  $\nu(Co-N)$ . Anal. Calcd. for  $C_{26}H_{20}N_4O_3K_2Cl_2Co$ : C, 48.45; H, 3.10; N, 8.69; Co, 9.15. Found: C, 47.23; H, 3.77; N, 9.93; Co, 9.40%.

**2.3.2.  $K_2[Co(HL_2)_2Cl_2] \cdot H_2O$  (C2).** C2 was prepared in a manner similar to that described for C1. Greenish brown powder, yield: 41.29%. IR (KBr disc,  $cm^{-1}$ ): 3436  $\nu(N-H)$ , 3155  $\nu(C-H)$ , 1625  $\nu(C=N)$ , 1550  $\nu(C=C)$ , 1245  $\nu(C-O)$ , 667, 597  $\nu(Co-O)$ , 424  $\nu(Co-N)$ . Anal. Calcd. for  $C_{26}H_{18}N_4O_3K_2Cl_4Co$ : C, 43.76; H, 2.52; N, 7.85; Co, 8.26. Found: C, 40.48; H, 1.83; N, 7.30; Co, 8.57%.

**2.3.3.  $K_2[Co(HL_3)_2Cl_2]$  (C3).** C3 was prepared in a manner similar to that described for C1. Light violet powder, yield: 43%. IR (KBr disc,  $cm^{-1}$ ): 3440  $\nu(N-H)$ , 3116  $\nu(C-H)$ , 1633  $\nu(C=N)$ , 1552  $\nu(C=C)$ , 1251  $\nu(C-O)$ , 671, 578  $\nu(Co-O)$ , 422  $\nu(Co-N)$ . Anal. Calcd. for

$C_{28}H_{22}N_4O_2K_2Cl_2Co$ : C, 51.38; H, 3.36; N, 8.56; Co, 9.01. Found: C, 57.05; H, 3.74; N, 9.41; Co, 10.30%.

**2.3.4. [Co(HL<sub>4</sub>)<sub>2</sub>] (C4).** C4 was prepared in a manner similar to that described for C1. Greenish brown powder, yield: 50%. IR (KBr disc,  $cm^{-1}$ ): 3419  $\nu(N-H)$ , 3056  $\nu(C-H)$ , 1625  $\nu(C=N)$ , 1550  $\nu(C=C)$ , 1242  $\nu(C-O)$ , 675, 534  $\nu(Co-O)$ , 457  $\nu(Co-N)$ . Anal. Calcd. for  $C_{26}H_{14}N_4O_2Cl_4Co$ : C, 50.73; H, 2.27; N, 9.10; Co, 9.58. Found: C, 49.34; H, 1.98; N, 8.87; Co, 9.28%.

**2.3.5. [Co(HL<sub>5</sub>)<sub>2</sub>] (C5).** C5 was prepared in a manner similar to that described for C1. Light brown powder, yield: 53%. IR (KBr disc,  $cm^{-1}$ ): 3431  $\nu(N-H)$ , 3058  $\nu(C-H)$ , 1625  $\nu(C=N)$ , 1548  $\nu(C=C)$ , 1249  $\nu(C-O)$ , 690, 553  $\nu(Co-O)$ , 478  $\nu(Co-N)$ . Anal. Calcd. for  $C_{30}H_{26}N_4O_2Co$ : C, 67.55; H, 4.87; N, 10.50; Co, 11.05. Found: C, 65.18; H, 4.51; N, 10.02; Co, 11.44%.

## 2.4. Computational details

DFT calculations were performed with the Gaussian 09 package using the B3LYP (hybrid GGA functional of Becke-Lee, Parr, and Yang [13,14]) level of theory, since as reported before, in the molecular simulation of transition metal containing systems better agreement with the experimental results can be obtained with this method [15-19]. In all cases, the electronic configuration of the molecular systems was described with the triple- $\zeta$  basis set augmented with one polarization functions of Ahlrichs and coworkers (TZVP keyword in Gaussian) [20]. For all the computed cobalt complexes, the quartet containing three unpaired electrons was the electronic ground state and thus open shell calculations were performed.

The vibrational frequency calculations were performed to ensure that the optimized geometries represent the global minima and that there are only positive eigen-values [21-23]. The optimized geometry of compounds furnished the total energy E.

## 2.5. General procedure for ethylene oligomerization

Ethylene oligomerizations and polymerizations were performed in a 1L stainless steel autoclave equipped with a mechanical stirrer and a temperature controller. Toluene, the desired amount of diethylaluminum chloride ( $Et_2AlCl$ ), and toluene solution of the catalyst precursor were added to the reactor in this order under a nitrogen atmosphere; the total volume was 110 mL. When the

desired reaction temperature was reached, ethylene at 20 atm pressures was introduced to start the reaction, and the ethylene pressure was maintained by a constant feed of ethylene during the reaction period. After 30 min, the reaction was stopped, and the autoclave was cooled. Then the pressure was released and a small amount of the reaction solution was collected, and the organic layer was analyzed as quickly as possible by gas chromatography (GC) to determine the composition and mass distribution according to GC spectrum of oligomers. Then the remaining reaction mixture was quenched with HCl-acidified ethanol (5%) in order to collect polyethylene obtained. However, the polyethylene was not formed.

### 3. Results and discussion

1*H*-Benzimidazol-2-yl-phenol derivatives (HL<sub>1</sub>–HL<sub>5</sub>) were prepared according to our reported procedures [13]. The cobalt (II) complexes were obtained by mixing the methanol solution of CoCl<sub>2</sub>·6H<sub>2</sub>O and the corresponding ligands with KOH at room temperature. The precipitation was immediately formed, which indicated the coordination of 2-(1*H*-benzimidazol-2-yl)-phenol to metal complexes is fast. The precipitation of the metal complexes were separated by filtration, washed with diethylether and dried in vacuum. The cobalt complexes (C1–C5) were obtained in good yields (43–62%). These complexes are stable in both solution and solid state. The analytical data and physical properties of the ligands and the cobalt complexes are summarized in table S1.

These compounds were characterized by FT-IR and UV-Vis spectra, ICP and elemental analysis (C, H and N). It has been tried hard in getting the single crystals of all complexes but the suitable crystals were not found in order to determine crystal structure of these compounds. Therefore, further investigation for direct molecular structures of complexes by DFT calculations was performed. Theoretical calculations involving geometry optimization, vibrational frequencies, stability of the compounds, <sup>1</sup>H- and <sup>13</sup>C-NMR spectra, as well as the various bond lengths and angles generated from the optimized structures have been done at the DFT/B3LYP level of theory.

#### 3.1. Geometrical parameters

The optimized geometry of HL<sub>2</sub> is shown in figure 1 as a representative ligand structure. The various bond lengths and angles generated from the structures of the optimized ligand (HL<sub>2</sub>) and

complex (**C2**) showed good resemble with the X-ray structural investigations of similar ligands and complexes reported [24-27]. The bond lengths and angles of the ligand ( $HL_2$ ) and complex (**C2**) are given in table 1. The optimized structure of **C2** is shown in figure 2.

### 3.2. FT-IR spectra

Vibrational properties of the ligands and complexes have been performed by using the DFT calculations with B3LYP/TZVP level. The prominent bands in the IR spectra of the cobalt complexes are presented in table S2.

For instance, the measured and calculated FT-IR spectra of the  $HL_2$  ligand and its related complex, **C2**, are compared in figure 3(a,b) and figure 4(a ,b), respectively. In the FT-IR spectra of **C1-C5**, the  $\nu(N-H)$  ( $\sim 1477\text{cm}^{-1}$ ),  $\nu(C=C)$  ( $\sim 1550\text{cm}^{-1}$ ),  $\nu(C=N)$  ( $\sim 1633\text{cm}^{-1}$ ) and  $\nu(C-O)$  ( $\sim 1251\text{cm}^{-1}$ ) bonds shifted to lower wavenumbers [28], in comparison with their corresponding free ligands  $HL_{1-5}$  ( $\nu(N-H) \sim 1490\text{cm}^{-1}$ ,  $\nu(C=C) \sim 1591\text{cm}^{-1}$ ,  $\nu(C=N) \sim 1637\text{cm}^{-1}$  [29] and  $\nu(C-O) \sim 1298\text{cm}^{-1}$ ), thereby indicating a coordinative interaction between the imino nitrogen atom and the central metal. Also,  $\nu(N-H)$ ,  $\nu(C=C)$ ,  $\nu(C=N)$  and  $\nu(C-O)$  in predicted theoretical spectra of the complexes are calculated at  $\sim 1480\text{cm}^{-1}$ ,  $\sim 1552\text{cm}^{-1}$ ,  $\sim 1633\text{cm}^{-1}$  and  $\sim 1255\text{cm}^{-1}$ , respectively. In the IR spectra of **C1-C5** complexes, the imine-nitrogen coordination could also be confirmed by appearance of a weak band located at the low wavenumbers ( $\sim 457\text{cm}^{-1}$ ), which may be assigned to (Co-N) [30, 31]. In the high frequency region, bands at  $2854\text{-}3180\text{cm}^{-1}$  are attributed to the stretching vibrations of aromatic  $\nu(C-H)$  for **C1-C5** complexes [32, 33], and the corresponding peaks in theoretical spectra are calculated at the range of  $3010\text{-}3172\text{cm}^{-1}$ . The sharp or medium bands in the complexes in the  $\sim 738\text{-}985\text{cm}^{-1}$  range are due to the out-of-plane deformation bands for the aromatic C-H [5]. In the IR spectra of **C1-C5** complexes, deprotonation and subsequent involvement of the phenoxyl group in metal coordination could also be supported by the appearance of new bands at a lower frequency ( $\sim 574, \sim 667\text{cm}^{-1}$ ) region assignable to (Co-O). These results are in agreement with the theoretical calculations. The experimental and calculated IR spectra of ligands and complexes agree extremely well with respect to their peak frequencies, the shapes of the bands, and band intensities [34].

### 3.3. UV-vis spectra

The UV-vis spectra of the ligands and the complexes were measured from 200-800 nm in DMSO and are given in table 2. According to the spectra, the lower-wavelength bands (210-300 nm) correspond to the  $\pi \rightarrow \pi^*$  transitions of the aromatic rings. The bands in the 310-360 nm region are due to  $n \rightarrow \pi^*$  transitions [9]. The electronic spectrum of **C1** shows a band at 360 nm related to  $L \rightarrow Co$  charge-transfer and two weak bands at 380 and 440 nm which may be assigned to  ${}^4T_{1g}(F) \rightarrow {}^4A_{2g}(F)$  and  ${}^4T_{1g}(F) \rightarrow {}^4T_{1g}(P)$  transitions, respectively.  ${}^4T_{1g}(F) \rightarrow {}^4T_{2g}(F)$  transition is not observed in the spectrum of the present complex. In most cases, it is rarely observed as it is inherently weak due to an orbital selection rule [35]. The spectra of **C2** and **C3** are like the spectrum of **C1**. They are characteristic for high-spin octahedral geometry for the **C1-C3** complexes. The electronic spectra of complexes **C4** and **C5** are of little help in the present case, since the  $d \rightarrow d$  transitions are masked by the strong charge-transfer bands [36]. In the electronic spectra of **C4** and **C5**, there is a band at 390 and 370 nm, respectively, that may be caused by the combination of oxygen  $\rightarrow$  metal, nitrogen  $\rightarrow$  metal charge-transfers ( $L \rightarrow Co$  charge transfer).

DFT theoretical studies of UV-vis spectra on the synthesized complexes were performed using the B3LYP/TZVP level of theory. The corresponding simulated absorption curves are plotted in figure 5 and the  $\lambda_{max}$  data are collected in table 2. As shown in figure 5, the calculated absorption spectra showed strong intense features around 400 and 390 nm for **C4** and **C5** and weak intense features around 390, 378 and 410 nm for **C1** to **C3**, respectively. Obtained  $\lambda_{max}$  values were in the range of the amounts obtained by UV-vis instrument.

### 3.4. NMR spectra of the ligands

${}^1H$ - and  ${}^{13}C$ - NMR data of the ligands are given in table 3. For instance, the  ${}^1H$  NMR spectra of **HL<sub>3</sub>**, **HL<sub>4</sub>** and **HL<sub>5</sub>** ligands exhibit only a broad singlet for the OH and the amine NH protons (13.14, 12.5 and 13.11 ppm for **HL<sub>3</sub>**, **HL<sub>4</sub>** and **HL<sub>5</sub>**, respectively). This combination results from strong intramolecular hydrogen bonding between the amine nitrogen with double bond and phenolic hydrogen atoms [37]. The **HL<sub>1</sub>** and **HL<sub>2</sub>** ligands give two singlets for OH and NH protons (13.07 ppm and 9.44 ppm for **HL<sub>1</sub>**, 13.26 ppm and 12.76 ppm for **HL<sub>2</sub>**, respectively). In the  ${}^1H$ -NMR spectra of **HL<sub>3</sub>** (having one methyl substituent at the 5-position on the benzimidazole ring) and **HL<sub>5</sub>** (having two methyl substituents at the 5,6-positions on the benzimidazole ring) show a singlet at 2.42 and 2.32 ppm, respectively. Position of protons and

the assignments of the peaks in benzimidazole moiety and phenolic ring moiety in HL<sub>1-5</sub> are different, the reason of this may be an electron donating (CH<sub>3</sub> substituents) or electron withdrawing group (Cl substituents) at the same position on the benzimidazole ring. It is known that the chloro groups on aromatic ring moves the resonance of the protons downfield, while the methyl groups on ring move the resonance of these protons upfield. <sup>1</sup>H-NMR spectra of the ligands are shown in figure S1. <sup>13</sup>C-NMR spectra of synthesized ligands were mentioned earlier. For example, in the <sup>13</sup>C-NMR spectrum of the HL<sub>1-5</sub> ligands, the signals at 157.71-158.98 ppm and 150.83-153.77 ppm are attributed to carbon atoms bonded to the OH oxygen atom and imidazole (C=N) carbon atom, respectively [5]. The low-signals of HL<sub>3</sub> and HL<sub>5</sub>, 21.29 ppm and 19.96 ppm, are due to methyl carbon atoms, respectively. The other signals are related to the benzimidazole and phenolic ring carbon atoms.

<sup>1</sup>H- and <sup>13</sup>C-NMR chemical shift calculations of the HL<sub>1-5</sub> ligands were carried out using the B3LYP/TZVP level of theory as used for geometry optimizations. The predicted <sup>1</sup>H- and <sup>13</sup>C-NMR chemical shifts were derived from the equation  $\delta = \Sigma o - \Sigma$ , where  $\delta$  is the chemical shift,  $\Sigma$  is the absolute shielding and  $\Sigma o$  is the absolute shielding of the standard (TMS) [38]. The chemical shift values obtained were compared with the experimental data listed in table 3. The results showed fair agreement between experimental and computed chemical shifts.

### 3.5. Thermodynamic stability calculation

The most important molecular orbitals are the frontier molecular orbitals, *i.e.* Highest Occupied Molecular Orbitals, HOMOs, and Lowest Unoccupied Molecular Orbitals, LUMOs. In fact, HOMO and LUMO energy gap determines the way the molecule interacts with other species. In other words, the frontier orbitals energy gap helps characterize the kinetic stability and chemical reactivity of the molecule so that the larger HOMO-LUMO gap always refers to lower chemical reactivity and higher kinetic stability [39]. The calculated HOMO-LUMO gaps of complexes **C1**, **C2**, **C3**, **C4** and **C5** at B3LYP/TZVP level of theory were 3.1, 3.0, 3.1, 3.8 and 3.9 eV, respectively. For these values we would say that although all the complexes are definitely stable, **C4** (figure 7) and **C5** (figure 6) show higher kinetic stability.

According to the geometry optimization of the structures of **C1-C3** with DFT calculations, Co is located on an octahedral center with the C=N nitrogen and hydroxy oxygen atoms of benzimidazole moiety and phenol ring, respectively, along with two chloride ions and

in complexes **C4** and **C5** is placed on a distorted tetrahedral center with one imine nitrogen and the phenolate oxygen atoms (molecular symmetry:  $D_{2h}$  for **C1-C3** and  $C_{2v}$  for **C4** and **C5**).

### 3.6. Ethylene oligomerization

At first, toluene was transferred to the fully dried reactor under a nitrogen atmosphere. The required amount of diethylaluminum chloride ( $Et_2AlCl$ ) as cocatalyst was then injected into the reactor via a syringe. Then, the desired cobalt complexes (10  $\mu$ mol) were suspended in toluene (10 mL). This mixture was transferred to a 1L Büchi laboratory autoclave under inert atmosphere and thermostated at 30 °C. An ethylene pressure of 20 bar was applied and the mixture was stirred for 30 min, then the ethylene flow was stopped. After cooling down, the ethylene pressure was carefully released. A sample (1 mL) was taken from the cooled mixture by syringe and applied for the GC analysis. The relative ratios of the oligomer fractions could be taken from the gas chromatogram. In all cases, these catalysts generate butenes and hexene as oligomeric products and the distribution of oligomers does not follow Schulz-Flory rules. No odd carbon number oligomers were detected in the GC analysis [40].

**3.6.1. Ethylene oligomerization by complexes C1-C5.** The catalytic activities of **C1-C5** for ethylene oligomerization have been carried out in the presence of  $Et_2AlCl$ . Complexes **C1** and **C2** produced  $C_4$  and  $C_6$ , whereas **C3-C5** produced  $C_4$  as main oligomeric product and showed high selectivity for 1-butene. Regarding the oligomer distribution, the bulkier R1, R2 substituents increase the content of  $C_4$  as given in table 4.

Their catalytic activities were significantly affected by the ligands environment, and their activity varied in the order  $C5 > C3 > C4 > C2 > C1$ . As it is clear, among the complexes, **C1** had the lowest catalytic activity and **C5** had the highest activity. The catalysts with electron-withdrawing group (**C2** and **C4**) showed lower activity than the catalysts with electron-donating group. This phenomenon is caused by the solubility factors of cobalt complexes. The complexes with ligands having additional methyl-substituents enhance their solubility, but complexes with ligands containing halides have lower solubility. The similar phenomena were also observed within complexes ligated by their analogues of the ligands [27].

Therefore, when the substituents were bulkier, cobalt pro-catalysts performed higher activity. It was believed that bulkier substituents might be helpful for both the solubility of complexes and stability of active species due to less exposure to impurity reactants [41].

Also, to clarify the correlation between the calculated effective net charge on the Co center and the observed activities of different complexes, NBO (Natural Bond Orbital) analysis was performed. In this regard, for all complexes, an electronic structure containing three unpaired electrons was considered since they showed lower energy values among other spin states. The values for NBO charges were varied from 0.944 to 0.951, 1.075, 1.064 and 1.087 for **C1** to **C5**, respectively. The variation trend between net charge and catalysis activity for synthesized complexes was predicted that their activities increase along with higher net charge on active center. This is in accordance with the finding of other authors [42, 43].

In addition, we compared our work with the literature [44-46]. In our work, bidentate ligands were used instead of tridentate, because bidentate ligands have high thermal stability and activity. Also, the oligomerization process is an exothermic reaction hence bidentate ligands due to high thermal stability are suitable for these reactions. But, in the literature, more tridentate ligands have been used.

As well as, in our work, the synthesized complexes could be easily activated with a low amount of cocatalyst ( $\text{Et}_2\text{AlCl}$ ) ( $\text{Al/Co} = 200$ ), and exhibited good activities and selectivity for ethylene oligomerization, while, in the literature, the amount of cocatalyst was very high ( $\text{Al/Co} = 1000$ ) in the ethylene oligomerization and even in the low amount of cocatalyst, activity was low.

Furthermore, in the present work, in the oligomerization process, wax or polymer was not formed at all and the final product is just oligomer and indicates that these catalysts are suitable for oligomer production. But, in the literature, in addition to oligomer, low amounts of polymers have been formed

#### **4. Conclusion**

Co(II) complexes containing 2-(2-hydroxyaryl)-1*H*-benzimidazole derivatives were synthesized and characterized. The structures of the ligands and complexes were characterized by FT-IR,  $^1\text{H}$ - and  $^{13}\text{C}$ -NMR and UV-vis spectra, ICP, and elemental analysis (C, H and N). All the analytical and spectral data are in agreement with theoretical calculations. According to the geometry

optimization obtained from DFT calculations, apart from **C4** and **C5** (with distorted tetrahedral geometry), all complexes are completed with two chloride ions adopting a six-coordinate octahedral geometry. Also, all complexes had the same number of three unpaired electrons and subsequently were in high spin. Also, for these catalysts essentially dimerization and trimerization were achieved, with a high selectivity for 1-butene and 1-hexene.

### Supplementary material

Cartesian coordinates of all the species discussed in the text together with spectral data for the synthesized ligands are available free of charge via the Internet at the publisher's website.

### Acknowledgements

This work was supported by Iran University of Science and Technology, Iran Polymer and Petrochemical Institute and Petrochemical Research & Technology Company. Naeimeh Bahri-Laleh thanks MOLNAC ([www.molnac.unisa.it](http://www.molnac.unisa.it)) for its computer facilities.

### References

- [1] W.H. Sun, S. Jie, S. Zhang, W. Zhang, Y. Song, H. Ma, J. Chen. *Organometallics*, **25**, 666 (2006).
- [2] W. Hang, Y. Weidong, J. Tao, L. Binbin, X. Wenqing, M. Jianjiang, H. You liang. *J. Chin. Sci. Bull.*, **47**, 616 (2002).
- [3] L. Xiao, R. Gao, M. Zhang, Y. Li, X. Cao, W.H. Sun. *Organometallics*, **28**, 2225 (2009).
- [4] W.H. Sun, S. Zhang, W. Zuo. *C. R. Chimie*, **11**, 307 (2008).
- [5] A. Tavman, I. Boz, A. Seher Birteksöz. *Spectrochim. Acta, Part A*, **77**, 199 (2010).
- [6] A. Tavman, S. Ikiz, A. Funda. Bagcigil, N. Yakutözgür, S. Ak. *Russ. J. Inorg. Chem.*, **55**, 215 (2010).
- [7] A. Tavman, S. Ikiz, A. Funda Bagcigil, N. Yakutözgür, S. Ak. *J. Serb. Chem. Soc.*, **74**, 537 (2009).
- [8] A. Tavman. *Transition Met. Chem.*, **32**, 172 (2007).
- [9] A. Tavman, I. Boz, A. Seher Birteksöz, A. Cinarli. *J. Coord. Chem.*, **63**, 1398 (2010).
- [10] A. Tavman, S. Ikiz, A. Funda Bagcigil, N. Yakutözgür, S. Ak. *J. Bull. Chem. Soc. Ethiop.*, **24**, 391 (2010).

- [11] M. Mao, Z. Wang, J. Li, X. Song, Y. Luo. *Synth. Commun.*, **40**, 1963 (2010).
- [12] N. DT, G. Atyam VSSS, R. Mi, S. Raidu. *J. Pharm. Chem.*, **2**, 273 (2010).
- [13] C. Lee, W. Yang, R.G. Parr. *J. Phys. Res, Part B*, **37**, 785 (1988).
- [14] A.D. Becke. *J. Chem. Phys.*, **98**, 1372 (1993).
- [15] F. Nouri-Ahangarani, N. Bahri-Laleh, M. Nekoomanesh-Haghighi. *Des. Monomers Polymers*, **19**, 394 (2016).
- [16] N. Bahri Laleh, A. Poater, L. Cavallo, S.A. Mirmohammadi. *Dalton Trans.*, **43**, 15143 (2014).
- [17] N. Bahri Laleh, M. Nekoomanesh Haghighi, S.A. Mirmohammadi. *J. Organomet. Chem.*, **719**, 74 (2012).
- [18] N. Bahri Laleh, L. Falivene, L. Cavallo. *Polyolefins J.*, **1**, 139 (2014).
- [19] A. Poater, L. Falivene, C.A. Urbina Blanco, S. Manzini, S.P. Nolan, L. Cavallo. *Dalton Trans.*, **42**, 7433 (2013).
- [20] A. Schäfer, H. Horn, R. Ahlrichs. *J. Chem. Phys.*, **97**, 2571 (1992).
- [21] S. Kundu, S. Biswas, A. Sau Mondal, P. Roy, T. Kumar Mondal. *J. Mol. Struct.*, **1100**, 27 (2015).
- [22] M.M. Ibrahim, A.M.M. Ramadan, H.S. El Sheshtawy, M.A. Mohamed, M. Soliman, S. Imam. *J. Coord. Chem.*, **68**, 4296 (2015).
- [23] R.C. Maurya, B.A. Malika, J.M. Mira, P.K. Vishwakarma, D.K. Rajaka, N. Jaina. *J. Coord. Chem.*, **68**, 2902 (2015).
- [24] Q. Shi, S. Zhang, F. Chang, P. Hao, W.H. Sun. *C. R. Chimie*, **10**, 1200 (2007).
- [25] L.L. Han. *Acta Cryst. E*, **E66**, o2047 (2010).
- [26] P. Hao, S. Zhang, W.H. Sun, Q. Shi, S. Adewuyi, X. Lu, P. Li. *Organometallics*, **26**, 2439 (2007).
- [27] X. Chen, L. Zhang, T. Liang, X. Hao, W.H. Sun. *C. R. Chimie*, **13**, 1450 (2010).
- [28] P.P. Hankare, L.V. Gavali, V.M. Bhuse, S.D. Delekar, R.S. Rokade. *Ind. J. Chem.*, **43**, 2578 (2004).
- [29] K. Kanmani Raja, N. Indra Gandhi, L. Lekha, D. Easwaramoorthy, G. Rajagopal. *J. Mol. Struct.*, **1060**, 49 (2014).
- [30] S.S. Qian, X.L. Zhao, L.H. Pang, Z.L. You, H.L. Zhu. *J. Coord. Chem.*, **42**, 345 (2016).
- [31] M.M. Abd Elzaher. *Appl. Organomet. Chem.*, **18**, 149 (2004).

- [32] N. Sundaraganesan, C. Meganathan, B. Anand, C. Lapouge. *Spectrochim. Acta, Part A*, **66**, 773 (2007).
- [33] C.A. Téllez S., A.C. Costa Jr., M.A. Mondragón, G.B. Ferreira, O. Versiane, J.L. Rangel, G. Müller Lima, A.A. Martin. *Spectrochim. Acta, Part A*, **169**, 95 (2016).
- [34] P. Saha, J. Prakash Naskar, A. Bhattacharya, R. Ganguly, B. Saha, S. Chowdhury. *J. Coord. Chem.*, **69**, 303 (2016).
- [35] K.K. Mohammed Yusuff, R. Sreekala. *Thermochim. Acta*, **179**, 313 (1991).
- [36] A. Tavman. *Transition Met. Chem.*, **31**, 194 (2006).
- [37] N. Sundaraganesan, B. Anand, F.-F. Jian, P. Zhao. *Spectrochim. Acta, Part A*, **65**, 826 (2006).
- [38] A.A. Dahy, E.S. Al-Farrag, N.S. Al-Hokbany, R.M. Mahfouz. *J. Coord. Chem.*, **69**, 1088 (2016).
- [39] M.A.M. El-Mansy, M.M. El-Nahass, N.M. Khusayfan, E.M. El-Menyawy. *Spectrochim. Acta, Part A*, **111**, 217 (2013).
- [40] X. Tang, W.H. Sun, T. Gao, J. Hou, J. Chen, W. Chen. *J. Organomet. Chem.*, **690**, 1570 (2005).
- [41] S. Song, R. Gao, M. Zhang, Y. Li, F. Wang, W. H. Sun. *Inorg. Chim. Acta*, **376**, 373 (2011).
- [42] W. Yang, Y. Chen, W.H. Sun. *J. Macromol. React. Eng.*, **9**, 473 (2015).
- [43] Y. Chen, W. Yang, R. Sha, R.D. Fu, W.H. Sun. *Inorg. Chim. Acta*, **423**, 450 (2014).
- [44] J. Ma, C. Feng, S. Wang, K. Q. Zhao, W. H. Sun, C. Redshaw, G.A. Solan. *Inorg. Chem. Front.*, **1**, 14 (2014).
- [45] S. Zhang, Q. Xing, W.H. Sun. *RSC Adv.*, **6**, 72170 (2016).
- [46] E. Yue, Y. Zeng, W. Zhang, Y. Sun, X.P. Cao, W.H. Sun. *J. Sci. China Chem.*, **59**, 1291 (2016).

## Figure captions

Figure 1. Optimized structure of HL<sub>2</sub> at B3LYP/TZVP level of theory.

Figure 2. Optimized structure of complex **C2** at B3LYP/TZVP level of theory.

Figure 3. The comparison of (a) experimental FT-IR, (b) theoretical IR, calculated at B3LYP/TZVP level, spectra for ligand HL<sub>2</sub>.

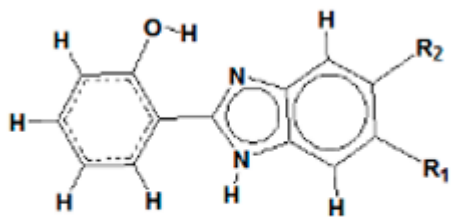
Figure 4. The comparison of (a) experimental FT-IR, (b) theoretical IR, calculated at B3LYP/TZVP level, spectra for complex **C2**.

Figure 5. Simulated UV-vis absorption spectra of the complexes at B3LYP/TZVP level of theory.

Figure 6. Optimized structure of complex **C5** at B3LYP/TZVP level of theory.

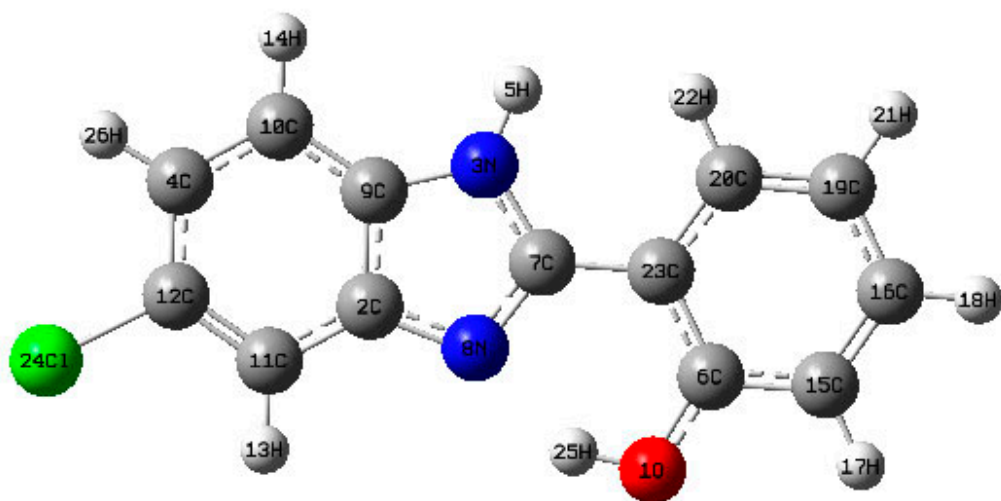
Figure 7. Optimized structure of complex **C4** at B3LYP/TZVP level of theory.

ACCEPTED MANUSCRIPT

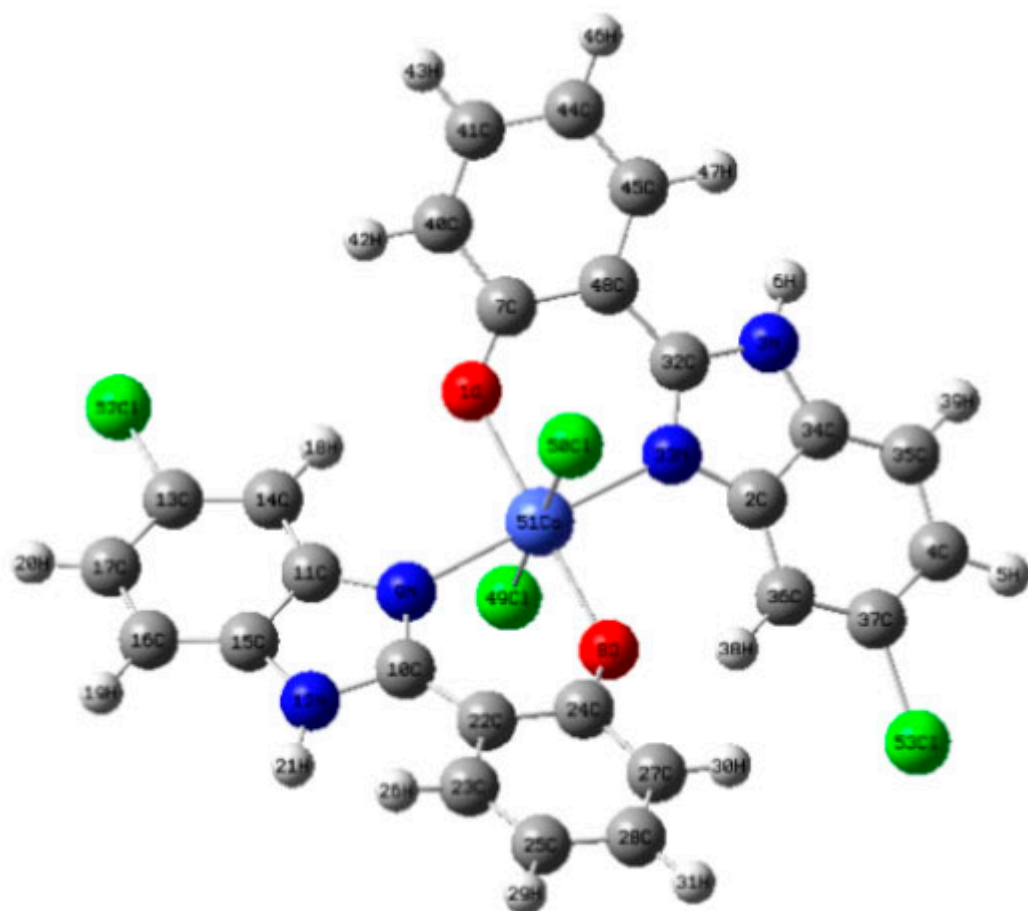


HL<sub>1</sub>: R<sub>1</sub> = R<sub>2</sub> = H  
HL<sub>2</sub>: R<sub>1</sub> = Cl, R<sub>2</sub> = H  
HL<sub>3</sub>: R<sub>1</sub> = CH<sub>3</sub>, R<sub>2</sub> = H  
HL<sub>4</sub>: R<sub>1</sub> = R<sub>2</sub> = Cl  
HL<sub>5</sub>: R<sub>1</sub> = R<sub>2</sub> = CH<sub>3</sub>

ACCEPTED MANUSCRIPT

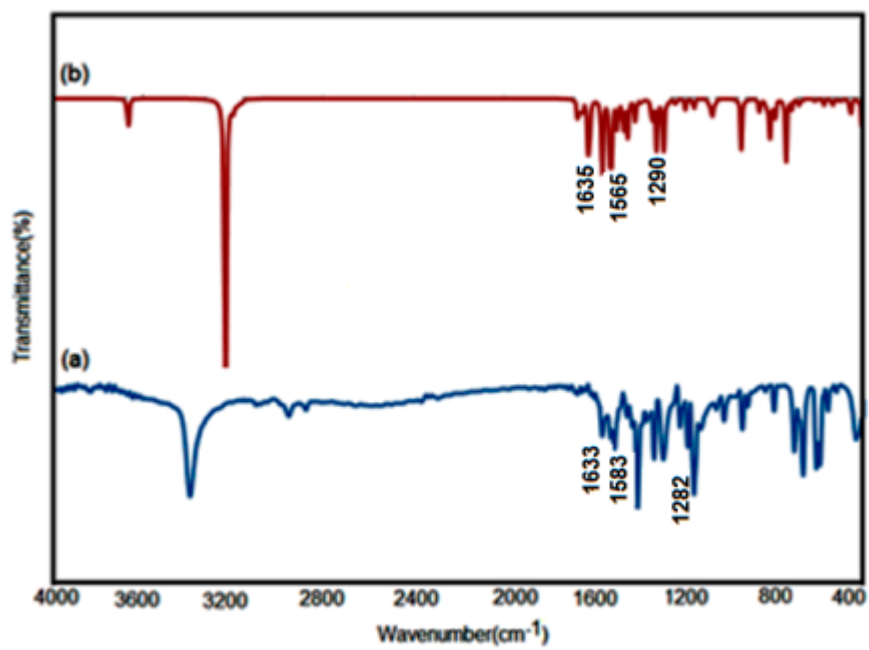


ACCEPTED MANUSCRIPT



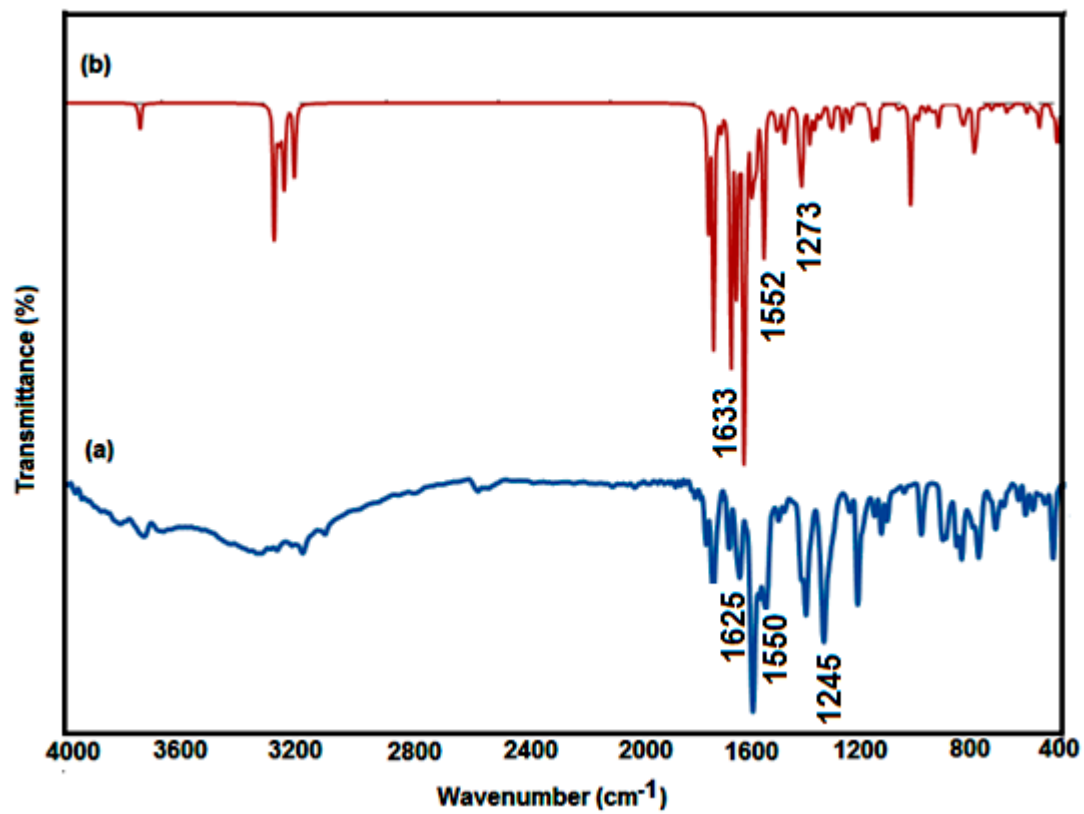
>

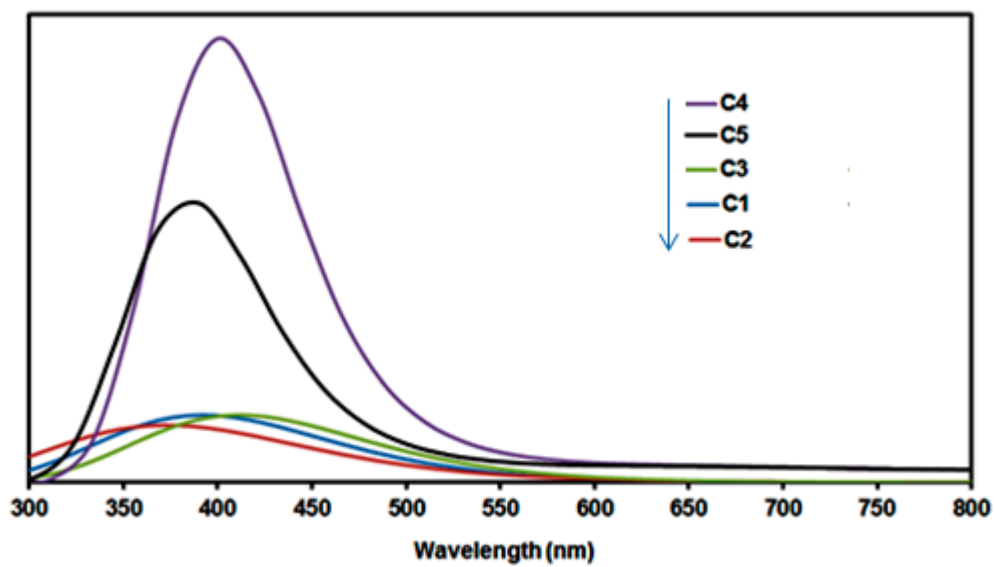
ACCEPTED



ACCEPTED MANUSCRIPT

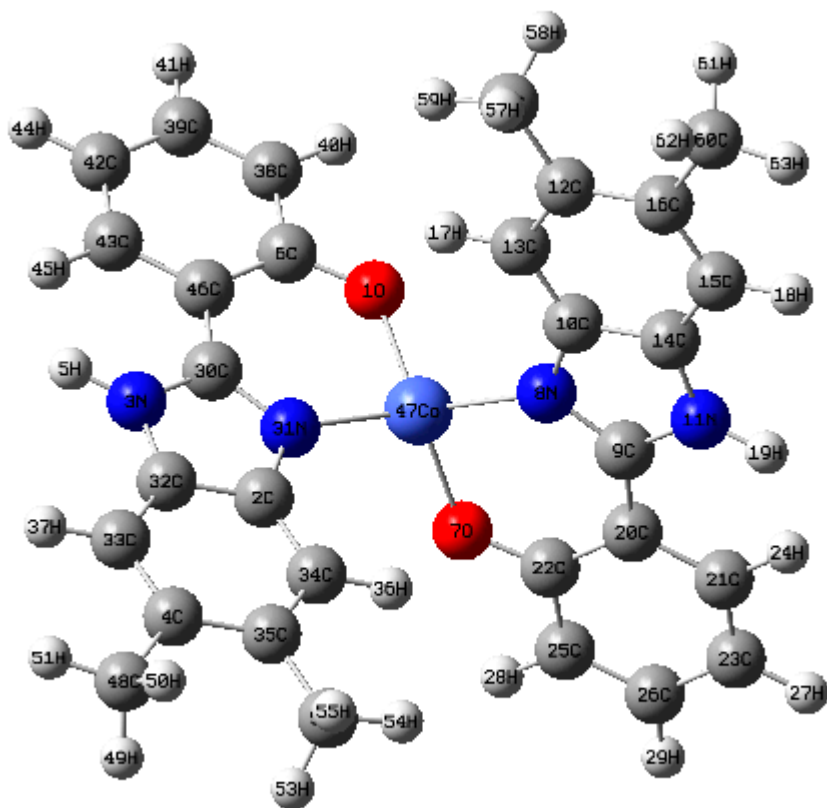
SCRIPT





ACCEPTED MANUSCRIPT

ACCEPTED MANUSCRIPT



ACCEPTED MANUSCRIPT

ACCEPTED MANUSCRIPT



Table 1. Selected bond lengths (Å) and angles (°) for HL<sub>2</sub> and C2.

HL <sub>2</sub>		C2	
<i>Bond lengths</i>			
O(1)-C(6)	1.341	Co(51)-O(1)	2.109
O(1)-H(25)	0.992	Co(51)-O(8)	2.109
N(3)-C(7)	1.375	Co(51)-N(9)	2.196
N(3)-C(9)	1.382	Co(51)-N(33)	2.196
N(8)-C(7)	1.323	Co(51)-Cl(49)	2.523
N(8)-C(2)	1.379	Co(51)-Cl(50)	2.513
<i>Bond angles</i>			
C(6)-O(1)-H(25)	108.69	N(9)-Co(51)-O(1)	95.60
C(7)-N(3)-C(9)	107.80	N(9)-Co(51)-O(8)	84.44
C(7)-N(8)-C(2)	106.51	N(9)-Co(51)-Cl(49)	88.66
N(8)-C(7)-N(3)	111.24	N(9)-Co(51)-Cl(50)	91.33
		N(9)-Co(51)-N(33)	177.32
		N(33)-Co(51)-O(1)	84.44
		N(33)-Co(51)-O(8)	95.60
		N(33)-Co(51)-Cl(49)	88.66
		N(33)-Co(51)-Cl(50)	91.33
		O(1)-Co(51)-O(8)	177.96
		O(1)-Co(51)-Cl(49)	91.02
		O(1)-Co(51)-Cl(50)	88.98
		O(8)-Co(51)-Cl(49)	91.01
		O(8)-Co(51)-Cl(50)	88.98
		Cl(49)-Co(51)-Cl(50)	179.99

Table 2. UV-vis spectra data of the compounds in DMSO.

Compound	UV (nm) (experimental)	vis (nm) (experimental)	vis (nm) (calculated)
HL <sub>1</sub>	250, 290	320	-
HL <sub>2</sub>	220, 240, 270, 290	310, 330	-
HL <sub>3</sub>	210, 240, 300	320, 340	-
HL <sub>4</sub>	300	340, 360	-
HL <sub>5</sub>	210, 240, 290	340	-
<b>C1</b>	-	360, 380, 440	390
<b>C2</b>	-	340, 380	378
<b>C3</b>	-	370, 390	410
<b>C4</b>	-	390	400
<b>C5</b>	-	370	390

Table 3. Theoretical assignment of  $^1\text{H}$ -NMR and  $^{13}\text{C}$ -NMR data for the ligands optimized by B3LYP/TZVP level: the chemical shift values ( $\delta_{\text{H}}$ , ppm).

Ligands	Proton assignment	$^1\text{H}$ -NMR (experimental)	$^1\text{H}$ -NMR (theoretical)	Carbon assignment	$^{13}\text{C}$ -NMR (experimental)	$^{13}\text{C}$ -NMR (theoretical)
HL <sub>1</sub>	NH	9.44	8.45	C=N	151.35	154.20
	OH	13.07	13.20	C-OH	158.98	167.80
HL <sub>2</sub>	NH	12.76	8.40	C=N	152.85	156.00
	OH	13.26	12.90	C-OH	157.87	168.00
				C-Cl	126.59	143.00
HL <sub>3</sub>	NH	13.14	8.35	C=N	151.40	154.00
	OH	13.14	13.20	C-OH	157.98	167.00
	CH <sub>3</sub>	2.42	2.50	C-CH <sub>3</sub>	131.54	137.00
				-CH <sub>3</sub>	21.29	21.00
HL <sub>4</sub>	NH	12.50	8.25	C=N	153.77	156.00
	OH	12.50	12.62	C-OH	157.71	167.70
				C-Cl	124.99	140.50
HL <sub>5</sub>	NH	13.11	8.30	C=N	150.83	153.80
	OH	13.11	13.20	C-OH	157.92	167.00
	CH <sub>3</sub>	2.32	2.35	C-CH <sub>3</sub>	131.31	136.00
				-CH <sub>3</sub>	19.96	20.10

Table 4. Results of ethylene oligomerization with **C1–C5**/ Et<sub>2</sub>AlCl<sup>a</sup>.

Entry	Precatalyst	Temperature (°C)	Al/C	Time (min)	Pressure (atm)	Yield (g)	Activity <sup>b</sup>	Oligomer distribution <sup>c</sup> (%)			
								C <sub>4</sub>	C <sub>6</sub>	α-C <sub>4</sub>	α-C <sub>6</sub>
1	<b>C1</b>	30	200	30	20	0.84	168	41.0	58.9	87.5	73.9
2	<b>C2</b>	30	200	30	20	2.30	460	96.6	3.33	93.1	100
3	<b>C3</b>	30	200	30	20	8.62	1724	100	-	100	-
4	<b>C4</b>	30	200	30	20	7.97	1594	100	-	100	-
5	<b>C5</b>	30	200	30	20	8.87	1774	100	-	100	-

<sup>a</sup> General conditions: 10 μmol precatalyst, 100 mL toluene as solvent; <sup>b</sup> In units of kg·mol<sup>-1</sup>·h<sup>-1</sup>; <sup>c</sup> Determined by GC. ΣC denotes the total amounts of oligomers.

